Journal of Petroleum Research and Studies

Open Access
Vol. 14, No. 4, December 2024, pp. 16-36

P- ISSN: 2220-5381
E- ISSN: 2710-1096

DOI: http://doi.org/10.52716/jprs.v14i4.882

Subsidence and Effective Stresses Distribution Using Finite Element Techniques for an Iraqi Oilfield

Ali K. Faraj[1,2*], Ameen K. Salih[1,2], Hassan A. Abdul Hussein[2], and Ali N. Abed Al-Hasnawi[3]

[1]Department of Petroleum Technology, University of Technology, Baghdad, Iraq
[2]Department of Petroleum Engineering, College of Engineering, University of Baghdad, Iraq
[3]Petroleum Research and Development Center, Ministry of Oil, Baghdad, Iraq
[*]Corresponding Author E-mail: 150103@uotecnology.edu.iq

Received 28/12/2023, Revised 27/03/2024, Accepted 02/04/2024, Published 22/12/2024

Abstract

Geomechanical problems are the most important problems that happen in the Zubair oil field; treating these problems requires a lot of time (Non-Productive Time) and thus increases the cost of drilling the well. Wellbore instability, subsidence, reservoir compaction, casing smash, pipe damage, and well kick is the main geomechanical problems facing the drilling process in the Mishrif formation, Zubair oilfield. The main goals of this study are to estimate the changes in stresses and subsequent subsidence values for this field during the production and injection periods. These estimation values, many problems can be avoided, thus increasing the drilling efficiency.

This study is to introduce the one way coupling between the reservoir model and geomechanical model using the finite element method. The finite element technique in CMG 2018 program was used to estimate the stress states during the production or injection operations in this field of interest.

The results of the 3D finite element model showed that the effective vertical stress rises by 32 psi during production while the effective horizontal stress increases by 16 psi. This may be explained by the fact that variations in pore pressure have little or no impact on the total vertical stress generated by weight. The results of this study demonstrated that the finite element method is a conservative method for coupling reservoir geomechanics and fluid flow. Subsidence values were 6.096 mm in the north part of the Al-Hammar dome, while at the center the subsidence was -5.1816 mm. Shuaiba dome has negative subsidence which is about -9.75 mm. It is important to note that the positive results subsidence signify the pore volume compacting, which may have an impact on the permeability and porosity of the reservoir petrophysics. As a result of a negative subsidence deformation, different failures including well casing damage, wellbore failure, and pipe

Open Access
Vol. 14, No. 4, December 2024, pp. 16-36

P- ISSN: 2220-5381
E- ISSN: 2710-1096

smashing, are expected. Based on these results, production can cause an increase in the differential stress, which leads to rock shear failure and in injection cases, increasing pore pressure can cause a tensile rock failure.

Keywords: Subsidence, Effective Stresses, Finite Element, Zubair oil field.

الهبوط وتقدير الإجهاد الفعال باستخدام تقنيات العناصر المحدودة لحقل نفط عراقي

الخلاصة:

تعتبر المشاكل الجيوميكانيكية من أهم المشاكل التي تحدث في حقل الزبير النفطي، تتطلب معالجة هذه المشاكل الكثير من الوقت (وقت غير منتج) وبالتالي يزيد من تكلفة حفر البئر. إن عدم استقرار حفرة البئر، وهبوطها، وانضغاط الخزان، وتحطم الغلاف، وتلف الأنابيب، وركل البئر هي المشاكل الجيوميكانيكية الرئيسية التي تواجه عملية الحفر في تشكيل مشرف، حقل الزبير النفطي. تتمثل الأهداف الرئيسية لهذه الدراسة في تقدير التغيرات في الضغوط وقيم الهبوط اللاحقة لهذا المجال خلال فترات الإنتاج والحقن. هذه القيم التقديرية، يمكن تجنب العديد من المشاكل، وبالتالي زيادة كفاءة الحفر.

تهدف هذه الدراسة إلى تقديم اقتران أحادي الاتجاه بين نموذج الخزان والنموذج الجيوميكانيكي باستخدام طريقة العناصر المحدودة. تم استخدام تقنية العناصر المحدودة في برنامج CMG 2018 لتقدير حالات الإجهاد أثناء عمليات الإنتاج أو الحقن في مجال الاهتمام هذا.

أظهرت نتائج نموذج العناصر المحدودة ثلاثية الأبعاد أن الضغط الرأسي الفعال يرتفع بمقدار 32 رطل/ بوصة مربعة أثناء الإنتاج بينما يزيد الضغط الأفقي الفعال بمقدار 16 رطل/ بوصة مربعة. يمكن تفسير ذلك من خلال حقيقة أن الاختلافات في ضغط المسام لها تأثير ضئيل أو معدوم على الإجهاد الرأسي الكلي الناتج عن الوزن. أوضحت نتائج هذه الدراسة أن طريقة العناصر المحدودة هي طريقة متحفظة لاقتران جيوميكانيكا الخزان وتدفق السوائل. كانت قيم الهبوط 6.096 ملم في الجزء الشمالي من قبة الحمر، بينما كان الهبوط في المركز -5.1816 ملم، اما قبة الشعيبة لها هبوط سلبي يبلغ حوالي -9.75 ملم. من المهم أن نلاحظ أن هبوط النتائج الإيجابية يدل على ضغط حجم المسام، والذي قد يكون له تأثير على نفاذية ومسامية الخزان الصخري. نتيجة لتشوه الهبوط السلبي، من المتوقع حدوث حالات فشل مختلفة بما في ذلك تلف غلاف البئر، وفشل حفرة البئر، وتحطم الأنابيب. بناءً على هذه النتائج، يمكن أن يتسبب الإنتاج في زيادة الضغط التفاضلي، مما يؤدي إلى فشل قص الصخور وفي حالات الحقن، يمكن أن يؤدي زيادة ضغط المسام إلى فشل الصخور الشد.

1. Introduction

The geomechanical research examines any deformation or failure that will occur on rocks as a result of production or injection, and it is a science that links the geology and mechanical characteristics of the rocks, [1]. The total and effective stresses vary as a result of the change in pore pressure during production or injection, which might result in various wellbore instabilities, understanding the state of these stresses requires combining reservoir models with geomechanical models, [2]. Wellbore instability types could be subsidence problems which may be porous compaction, pipe harm, well casing smash, and tensile or failure of the borehole, [3,4]. Wellbore instability also results from azimuth and inclination when drilling at a more horizontal or deviated hole, [5]. Conducting an analysis of the mechanical properties variation of the rock is imperative

Open Access
Vol. 14, No. 4, December 2024, pp. 16-36

P- ISSN: 2220-5381
E- ISSN: 2710-1096

to mitigate potential issues related to instability within the well bore, [6], so wellbore stability is one of the main steps in the drilling design of wells, [7, 8, 9].

A calculating technique called the finite element method is utilized to get the best answer for current issues. Usually, during reservoir production, pore pressure depletion causes an increase in effective vertical stress, which leads to rock deformation. Porosity and permeability variations brought on by rock deformation have an impact on reservoir production, [2]. The structural components of the reservoir are first divided into tiny units called elements, which are then assembled to form a mesh, as part of the finite element procedure, [10].

Over the last years, a large number of reputable oil producers in addition to lone researchers have carried out more in studies into the issue of reservoir compaction and subsequent subsidence. Several field studies on reservoir compaction and subsidence issues have been seen like Goose Creek region near Galveston, Texas [11]; California's Wilmington Oil field is located in Long Beach [12, 13]; California's Los Angeles Inglewood fields [14]; the oil fields along the Bolivar Coast of Lake Maracaibo in Venezuela [15]; the Groningen gas field in the Netherlands [16]; the Nigata gas field [17]; the Po river delta gas producing area in Italy [18]; and the Ekofisk Field in the North Sea [19].

Subsidence can range from a few millimeters to several meters in several instances. Despite the rarity of these events, they have the potential to cause severe environmental and technical issues. Porosity and permeability are two reservoir petrophysical characteristics that might be affected by subsidence issues. On the other side, reservoir compaction can function as an active driving mechanism and, as a result, affect the reservoir's recovery. This study was first presented at the first effective stresses and the subsequent subsidence estimation in the Zubair oil field. a geomechanical model and reservoir model that are linked together to forecast the level of stress during production or injection over a certain time period.

2. Area of Study

The Zubair Field was selected for investigation. As can be observed in Figure (1), it is one of the overripe oil fields in the southern area of Iraq, situated about 20 kilometers southwest of Basra city, [20]. From northwest to southeast, the Zubair Field is separated into four domes by saddles (Al-Hamar, Shuaiba, Rafidyah, and Safwan). According to Iraq's tectonic zones, the Zubair oilfield is

Open Access
Vol. 14, No. 4, December 2024, pp. 16-36

P- ISSN: 2220-5381
E- ISSN: 2710-1096

located in the sagging pelvis of the Mesopotamian zone, which is a section of the Arabian plate's quasiplatform foreland, [21]. The Euphrates subzone, Tigris subzone, and Zubair subzone are the three subzones of the Mesopotamian. The study region is located within the Zubair subzone. The Alpine orogenic motions (basement faults and salt formations) make the Zubair subzone unstable. These elements are to blame for the formation of subsurface anticline structures in Iraq's southern regions, [22]. Figure (2) shows how the Zubair oilfield's geological stratigraphic column is characterised by a thick sequence of Cretaceous carbonates that include significant and numerous hydrocarbon accumulations.

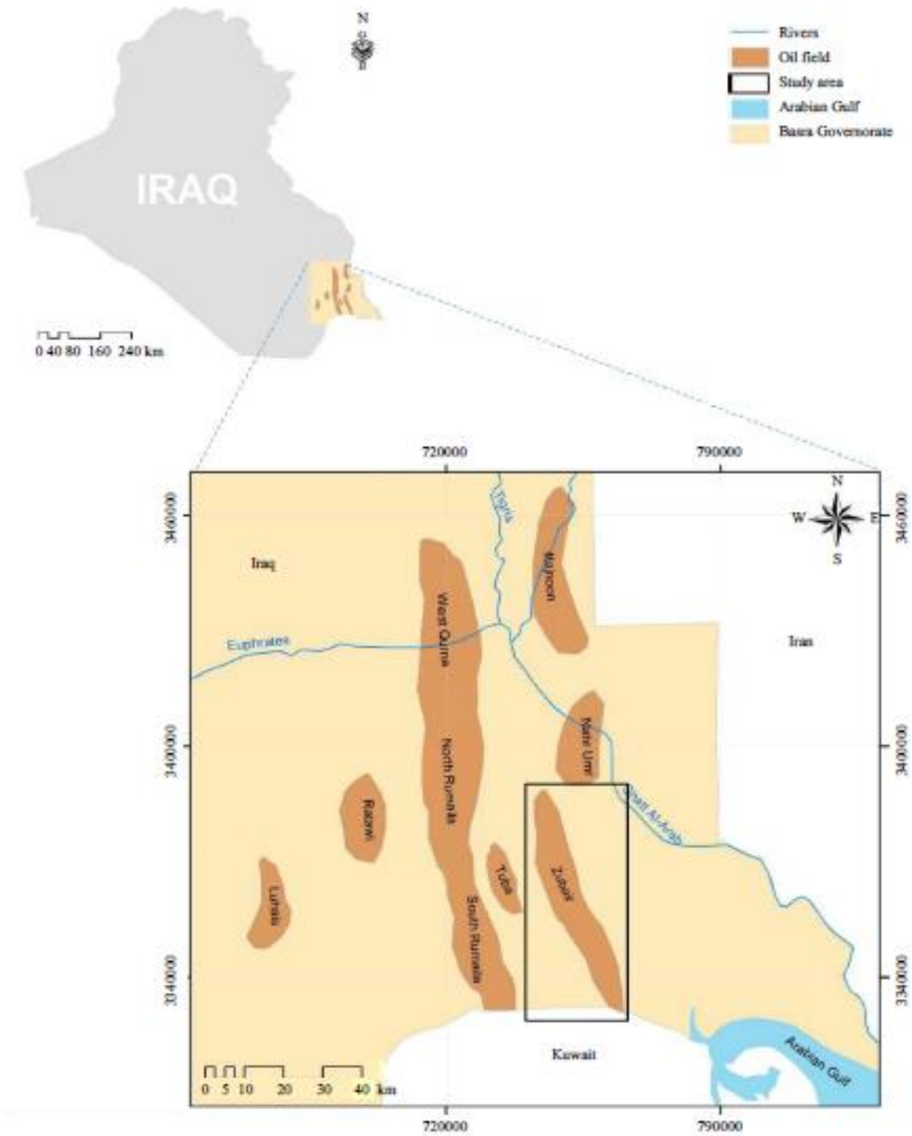

Fig. (1): Zubair oilfield map, [23].

Open Access
Vol. 14, No. 4, December 2024, pp. 16-36

P- ISSN: 2220-5381
E- ISSN: 2710-1096

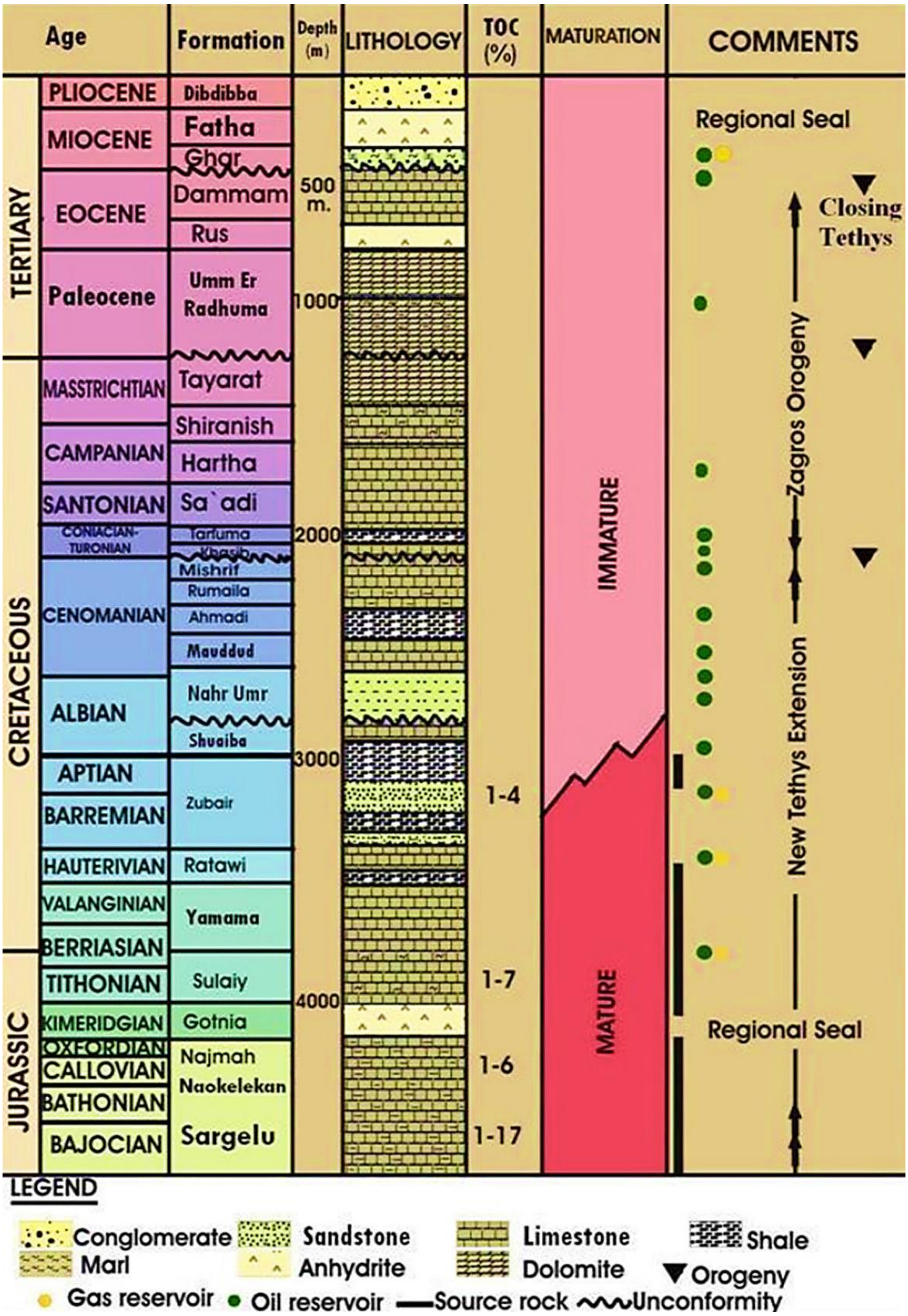

Fig. (2): Stratigraphic Column of Zubair Oilfield, [24].

Open Access
Vol. 14, No. 4, December 2024, pp. 16-36

P- ISSN: 2220-5381
E- ISSN: 2710-1096

3. Finite Element Method

The three-dimensional element is in coordinate with the dimensions dx, dy, and dz, with normal and shear stress, as illustrated in Figure (3). The letters x, y, and z stand for shear stresses, which act in the planes of the element, whereas the letters y, x, and z stand for normal stresses, which are perpendicular to the element's face.

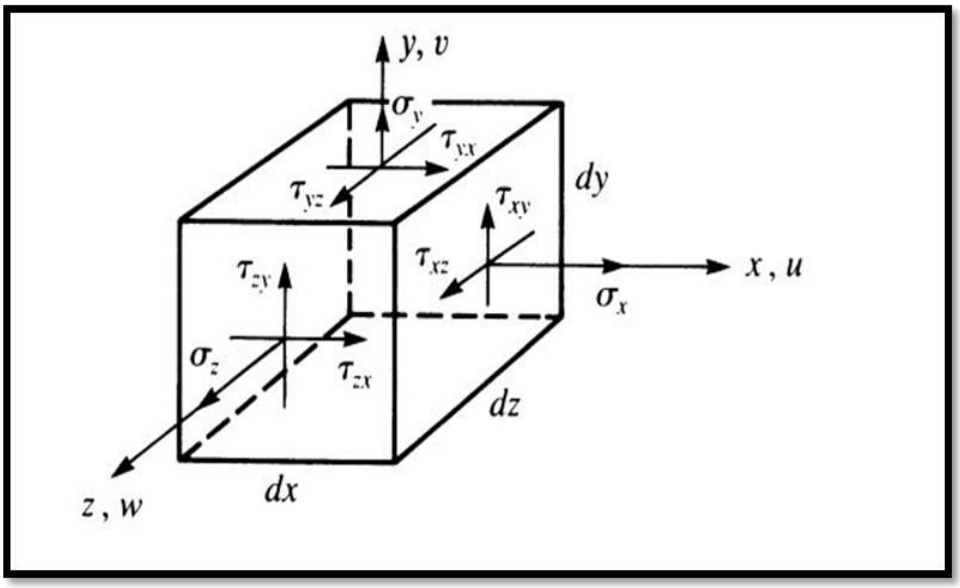

Fig. (3): Three –dimension stresses on element.

The finite element methodology provides two direct ways for resolving structural mechanical problems. First Strategy internal force, sometimes known as flexibility or force, was used as an unidentified component in some ways. The second strategy, sometimes referred to as the stiffness or displacement approach, assumes that node displacement is unknowable. The stiffness approach is more practical since the formulation of most structural systems is simple [25].

3.1 Weak Galerkin Method

These Terzaghi effective stress is the vector of the total stress component and the pore pressure at any location of the poroelastic medium, [26,27].

$$\sigma^{\wedge} = \sigma - P \tag{1}$$

Where $\sigma^{\wedge}$ is effective stress in (psi) units, σ is the total stress and P is the pore pressure.

Open Access
Vol. 14, No. 4, December 2024, pp. 16-36

P- ISSN: 2220-5381
E- ISSN: 2710-1096

The least-squares finite element method is used to solve numerical partial differential equations. Finite element techniques based on least squares have been developed for solving the Stokes and Navier equations, as well as for elasticity, in second order elliptic situations. [28, 29, 30, 31]. However, the majority of the available least-squares finite element techniques include limits on the choice of approximation functions and the underlying finite element partitions because of the consistency requirement, [32]. The finite element technique offers flexibility in mesh creation and the construction of finite element functions due to discontinuous approximations. A novel finite element technique called the weak Galerkin method, published employs discontinuous polynomials on a polytopal mesh as shown in equation (2), [2].

$$K\frac{du}{dt} + Lw\,\frac{dP_w}{dt} + Lo\frac{dP_o}{dt} + Lg\frac{dP_g}{dt} - \frac{df}{dt} = 0 \qquad (2)$$

Where K is stiffness matrix, u is displacement vector, L is coupling matrix between mechanical and fluid flow, (Pw, Po and Pg) is pore pressure and F vector of boundary condition.

3.2 Subsidence

Subsidence is the word used to describe when a surface point sinks to a lower level or when the earth sinks and carries a thing with it. Subsidence may be induced by geological factors such as tectonic or volcanic activity, material removal from below the surface, tunneling, fluid movement, or natural forces like as a sink hole in a limestone region, [33]. Equation (3) can be used to calculate subsidence, [34].

$$S_{(p,t)} = \sum_{k=1}^{N} f(r_k\,, P)\, A_k b_k\, P_k(t) \qquad (3)$$

Where S is subsidence, N is the number of elements which reservoir subdivided, Pk(t) is the pressure drop at time of element k, Ak cross section area and bk is vertical thickness.

4. Methodology

Data was collected from production wells (ZA-2, ZA-3, and ZA-44), as well as injection wells (ZA-24 and ZA-36), in the north section of the Zubair oil field, which includes two domes (Shuaiba and Al-Hamar). The computer modeling Group (CMG 2018) finite element analysis software was utilized to distribute and analyze stresses for all field regions throughout the production or injection operations.

Open Access
Vol. 14, No. 4, December 2024, pp. 16-36

P- ISSN: 2220-5381
E- ISSN: 2710-1096

The fluid flow model was used to calculate the depletion in formation pressure due to production and the increase in pore pressure due to injection. The stress distribution was computed using a geomechanical model. Typically, reservoir models do not account the variations in reservoir stress, thus these two models must be coupled.

This coupling model was developed by create components for the flow model, such as maximum pressure, temperature, oil density, gas gravity, and bubble point pressure. Make a rock fluid type (oil-water and liquid-gas) that includes relative permeability and saturation. Insert the initial conditions for the three-phase containment of water, oil and gas with the contacts of (water-oil and gas-oil). Geomechanics data such as total stresses at the starting point including (vertical stress, minimum and maximum horizontal stresses). 3D finite technique, one-way coupled model, Young's modulus, frictional angle, Poisson ratio, and cohesiveness were all included in the elasto-plastic Mohr-Coulomb model, list of boundary conditions.

In the context of the project's specifications, the designated dimensions were established as follows: 24200 meters in the x-direction, 33600 meters in the y-direction, and 1128.3696 meters in the z-direction. The overall grid was comprised of a total of 23 columns, 33 rows, and 6 layers, denoted as nI, nJ, and nK respectively. In 2014, the project encompassed the initiation of production and injection wells.The recommended temporal increment for the project was set at an interval of eight years, commencing in 2014 and concluding in 2022. The envisaged daily production rate stood at approximately 9000 barrels, while the corresponding daily injection water rate was determined to be 42000 barrels.

5. Results and Discussion

5.1 Effective Horizontal Stress

Figure (4) depicts the distribution map of effective horizontal stress for the Mishrif formation. The map shows a decrease in effective horizontal stresses at injection wells, whereas effective horizontal stresses are increased at production wells and the area around these wells. Pore pressure change effect on the total horizontal stresses which led to a small increase in the effective horizontal stresses. The total horizontal stress decreases more quickly at the beginning of production, the effective horizontal stress in well ZA-2 increased quicker on the 60th day rising by around 4 psi from 10500 psi to 10504 psi as shown in Figure (5). Then, after eight years, the stress gradually increased until it reached 10516 psi. The effective horizontal stress in the injection

Open Access
Vol. 14, No. 4, December 2024, pp. 16-36

P- ISSN: 2220-5381
E- ISSN: 2710-1096

well ZA-24 is seen in Figure (6) to be decreasing over time to 10490 psi. Because total horizontal stress increases with increasing of pore pressure and the inverse relationship between total stress and effective horizontal stress, effective stress drops as pressure increases.

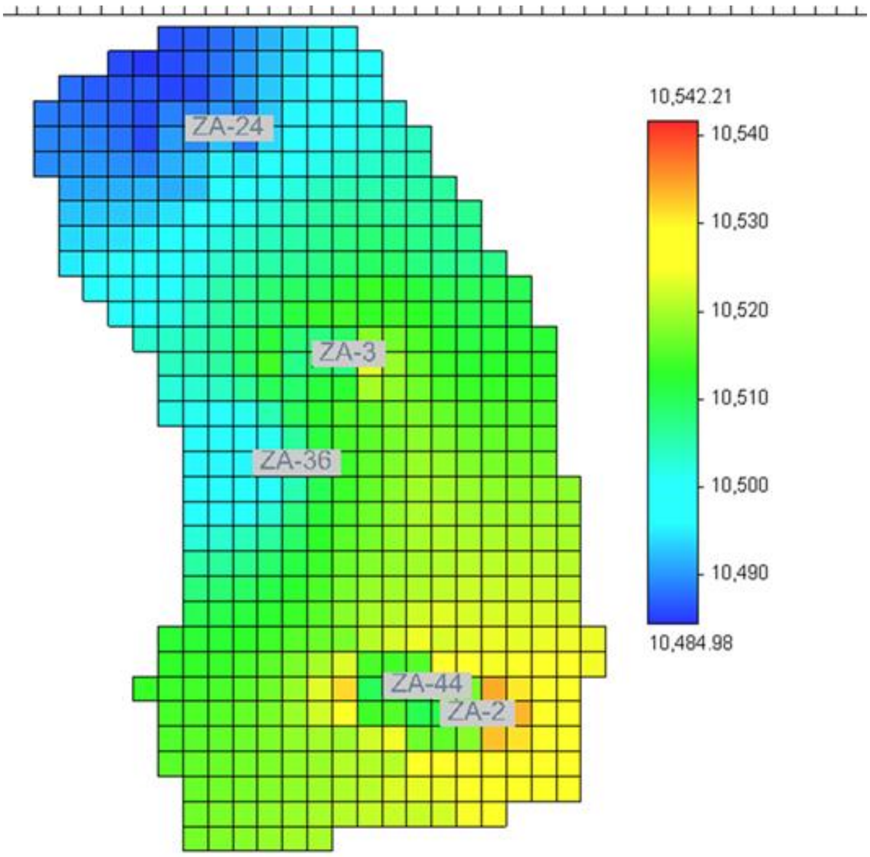

Fig. (4): Effective horizontal stress distribution map for Mishrif formation.

Open Access
Vol. 14, No. 4, December 2024, pp. 16-36

P- ISSN: 2220-5381
E- ISSN: 2710-1096

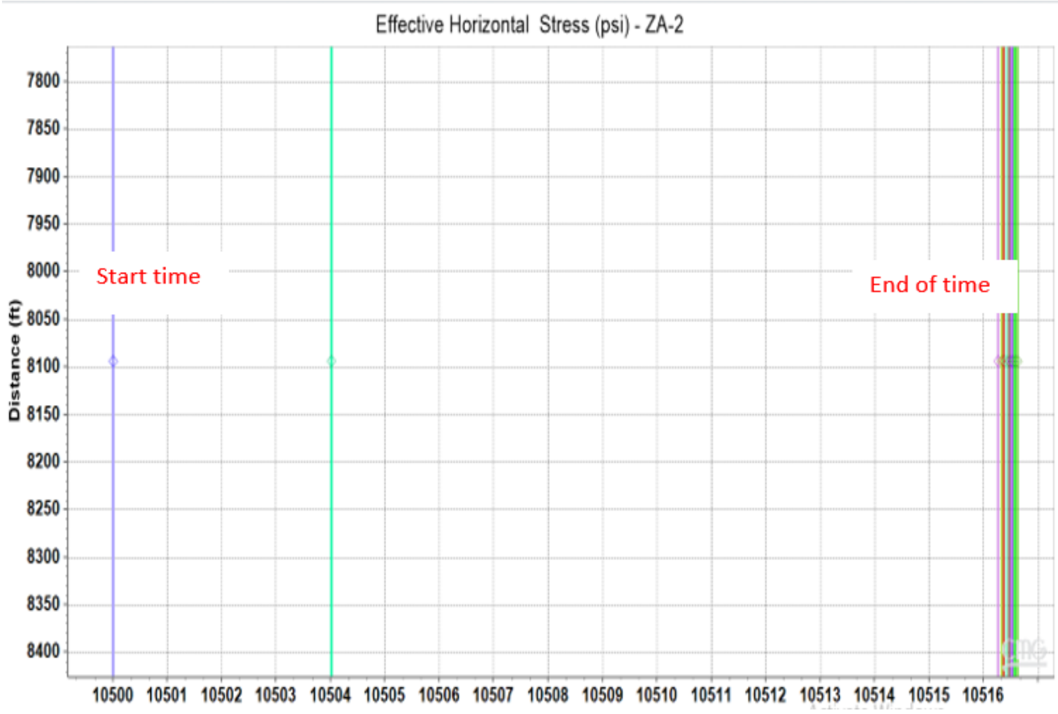

Fig. (5): Effective horizontal stress at different time step for well ZA-2.

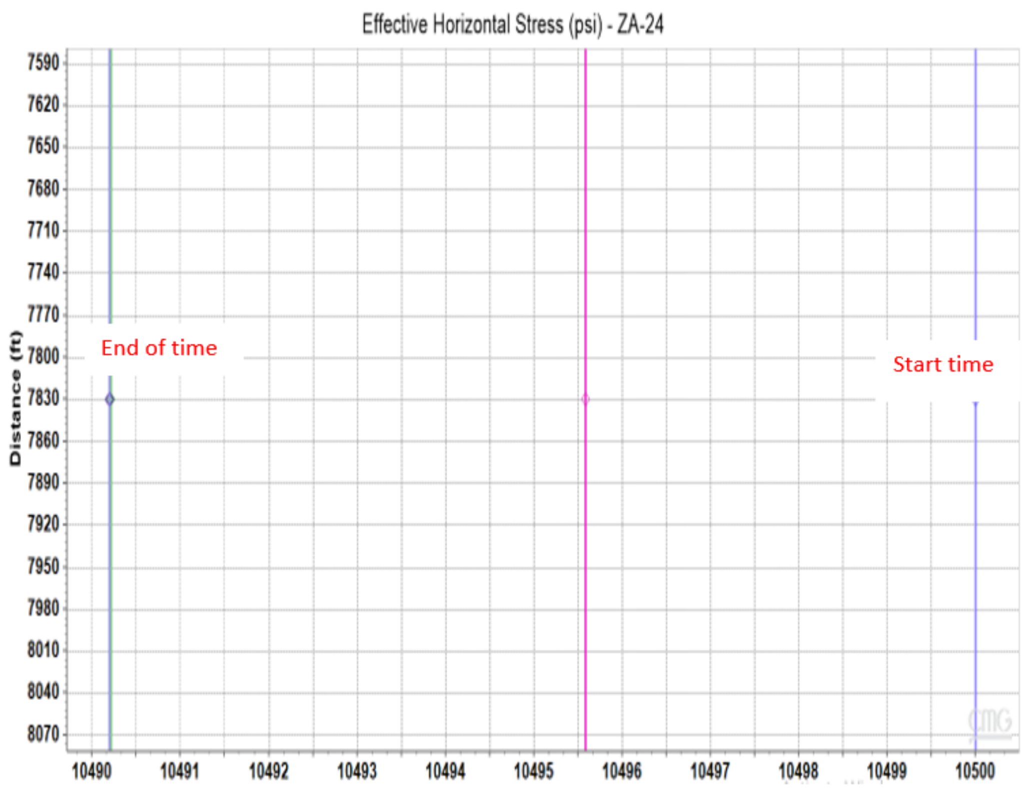

Fig. (6): Effective horizontal stress at different time step for well ZA-24.

Open Access
Vol. 14, No. 4, December 2024, pp. 16-36

P- ISSN: 2220-5381
E- ISSN: 2710-1096

5.2 Effective Vertical Stress

The distribution map of effective vertical stress (σv-P) in the Mishrif formation is shown in Figure (7) below. As formation pressure reduced, the effective vertical stress increased. As a result, the differential stress may rise, leading in rock shear collapse. Because of the injection processes led to an increase in pore pressure, the differential stress dropped, resulting in tensile failure [35]. As shown in Figure (8), effective vertical stress during production and pressure depletion increases more quickly from the first 60th day, then continuously increase to 4032 psi at the end of the time step. As can be seen, the effective horizontal increasing in production well (ZA-2) from 10500 psi to 10516 rises by 16 psi, while the effective vertical stress rises by 32 psi in the same well. This can be explained by the fact that the total vertical stress produced by weight is unchanged by changes in pore pressure, effective vertical stress increases more quickly during pore pressure depletion, according to poroelastic theory, while total horizontal stress drops with pore pressure, effective horizontal stress increases more slowly than pore pressure decreases. The pore pressure increased more quickly at the start of the injection, leading the effective vertical stress to decline even faster, from 4000 psi on the 60th day to 3990 psi at the end of the time step, as shown in Figure (9).

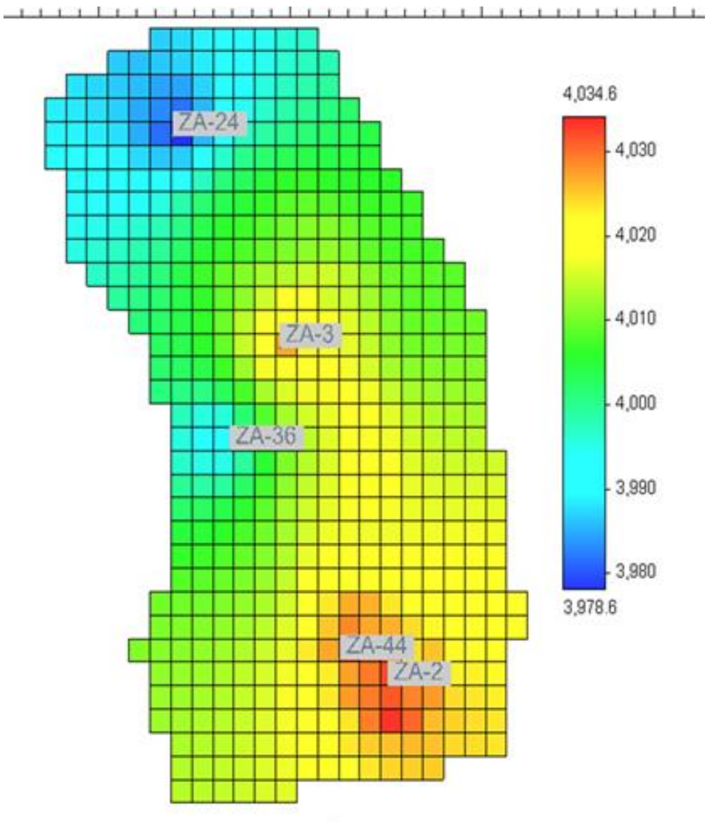

Fig. (7): Effective vertical stress distribution map in Mishrif formation after 8 years.

Journal of Petroleum Research and Studies

Open Access
Vol. 14, No. 4, December 2024, pp. 16-36

P- ISSN: 2220-5381
E- ISSN: 2710-1096

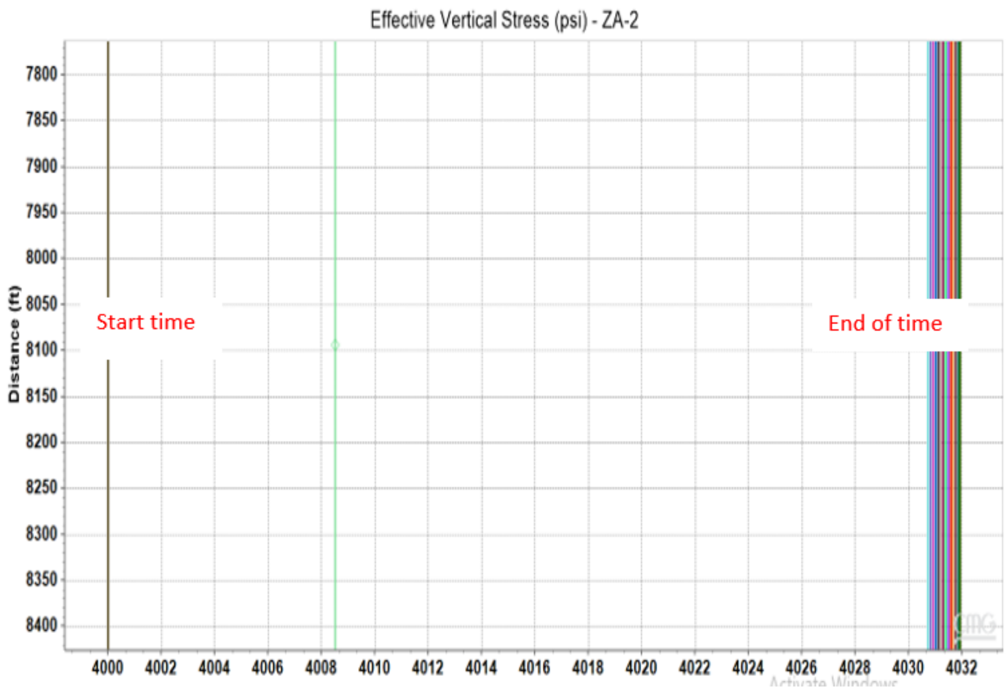

Fig. (8): Effective vertical stress at different time step for well ZA-2

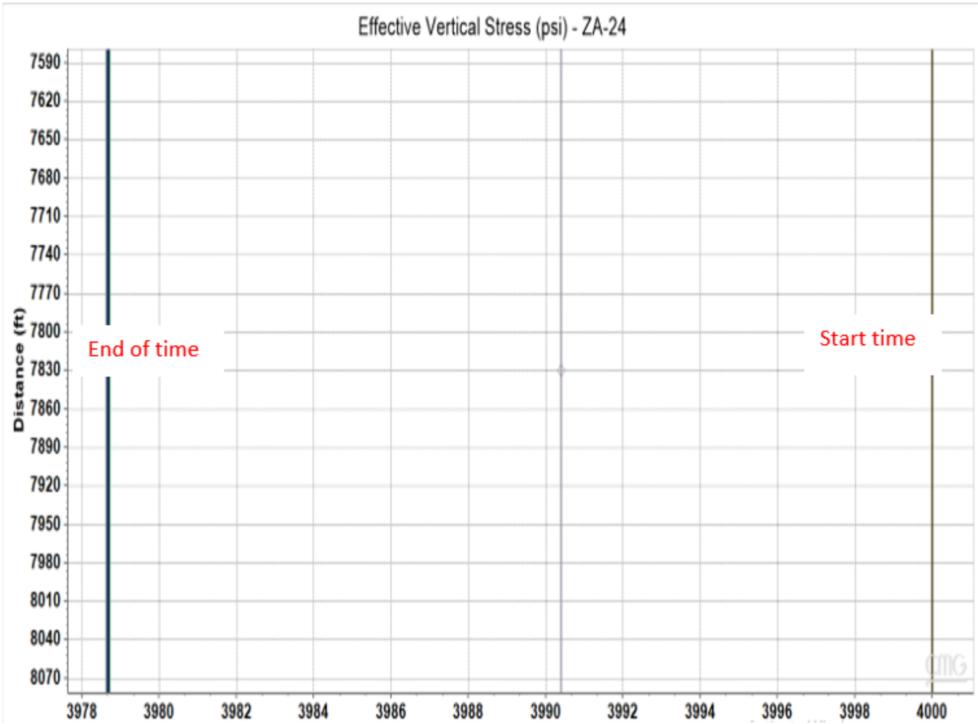

Fig. (9): Effective vertical stress at different time step for well ZA-24.

Open Access
Vol. 14, No. 4, December 2024, pp. 16-36

P- ISSN: 2220-5381
E- ISSN: 2710-1096

5.3 Subsidence by Geomechanics

Subsidence from geomechanical reasons is another significant issue that may occur during production as a result of fluid movement, as seen in Figure (10). The subsidence values of the injection wells were positive, but the subsidence values during production were negative. Figure (11) findings for well ZA-2 subsidence show that during the first 60th day, the subsidence increased more quickly to negative values of approximately -0.01 ft (-3.048 mm), then continued to increase steadily after 8 years from prediction start, at about 0.032 ft (-9.75 mm). The increase in both vertical and horizontal effective stress is what caused this. According to Figure (12), ZA-24 exhibits a faster increase in positive values of subsidence from zero mm to 0.011 ft (3.3528 mm) at the first 60th day, followed by an increasing to 0.02 ft (6.096 mm) after eight years.

Positive subsidence values indicate pore volume compacting and rock deformation, this may affect reservoir petrophysical properties like porosity and permeability. Negative subsidence values at the Shuaiba and Al-Hammar domes may cause well casing damage, wellbore failure, and pipe smash, [3].

Open Access
Vol. 14, No. 4, December 2024, pp. 16-36

P- ISSN: 2220-5381
E- ISSN: 2710-1096

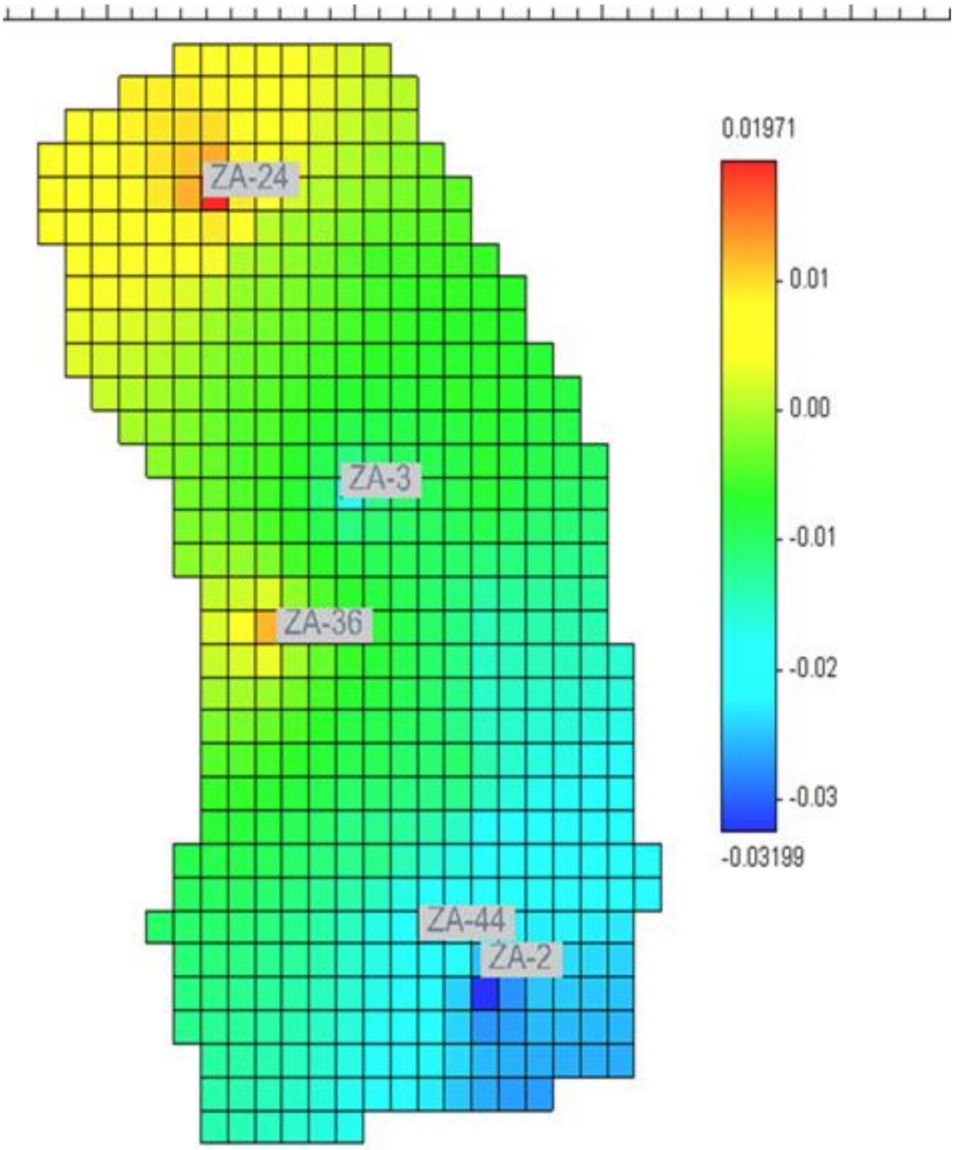

Fig. (10): Subsidence from geomechanical map for Mishrif formation.

Open Access
Vol. 14, No. 4, December 2024, pp. 16-36

P- ISSN: 2220-5381
E- ISSN: 2710-1096

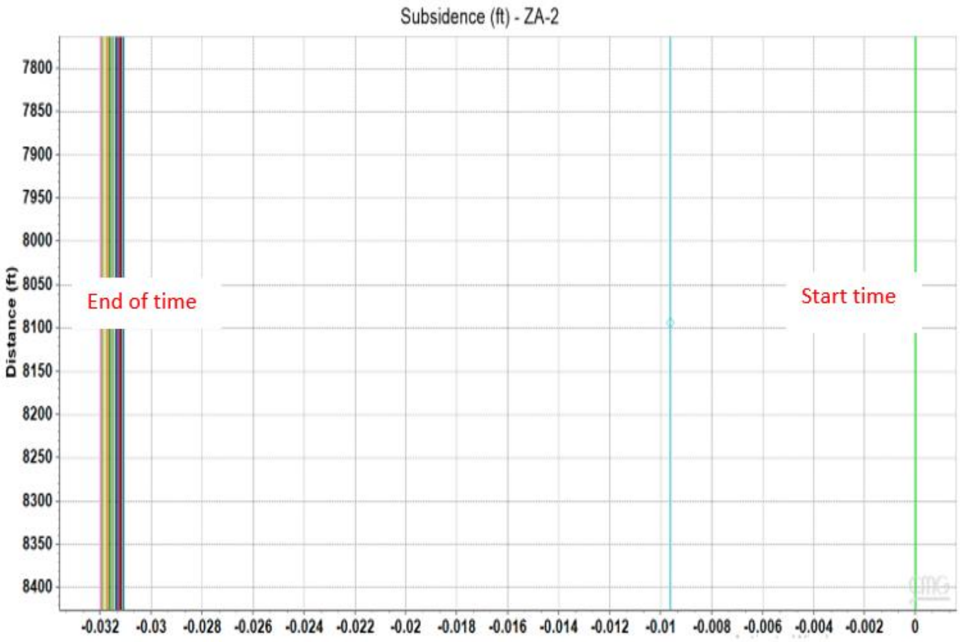

Fig. (11): Subsidence from geomechanics for different time step in ZA-2 well.

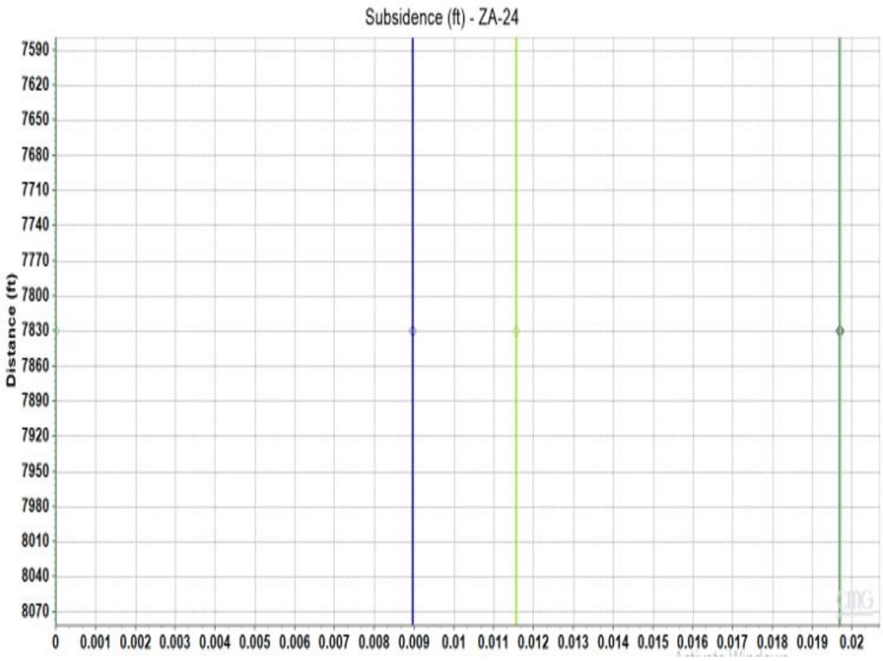

Fig. (12): Subsidence from geomechanics for different time step in ZA-24 well.

5.4 Relationship Between Subsidence and Effective Stress

The effective stress and subsidence have inverse relationships, as indicated by the findings in Figures (13), and (14). The subsidence tends to decrease toward negative values when the

Open Access
Vol. 14, No. 4, December 2024, pp. 16-36

P- ISSN: 2220-5381
E- ISSN: 2710-1096

effective stress rises as a result of production, which might cause formation to creep toward the pipe or casing and smash it. The effective stress will decrease when pore pressure rises during well injection, which causes the subsidence to rise toward positive values, indicating rock deformation. Drilling wells in areas with low rates of subsidence is the best way to avoid these issues.

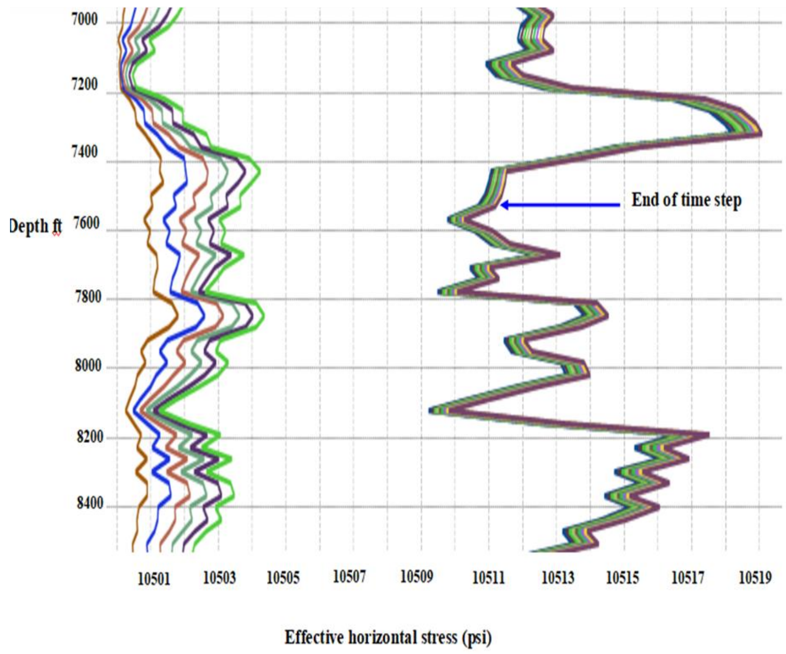

Fig. (13): Effective horizontal stress in Mishrif formation for the Zubair oil field.

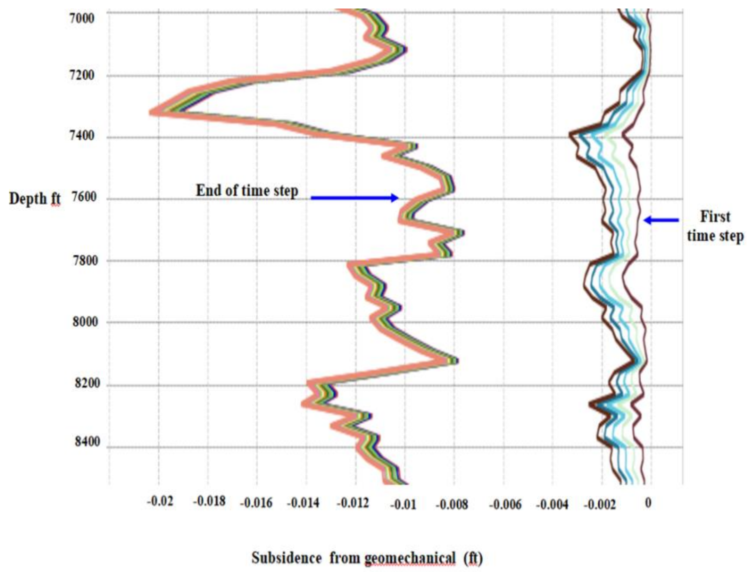

Fig. (14): Subsidence in Mishrif formation for Zubair field.

Open Access
Vol. 14, No. 4, December 2024, pp. 16-36

P- ISSN: 2220-5381
E- ISSN: 2710-1096

6. Conclusions

Based on the obtained results from the previous section, the following conclusions can be drawn as follows:

- The results of current model showed that, the finite element analysis can be considered as a good tool for geomechanical modeling, it's the future of the industry.
- Tensile failure may occur due to a decrease in effective stresses during the injection of water. Shear failure may be happened when the effective stresses increase, according to a finite element distribution.
- Due to negative subsidence values in the Shuaiba dome, well casing damage, wellbore failure, and pipe smash are all anticipated issues. The effective vertical stress changes during the production and injection phases, indicating compaction and deformation in the reservoir rock.
- According to model results, effective vertical stress rises higher than effective horizontal stress because variations in pore pressure have no effect on the values of the total vertical stress created by weight.

Open Access
Vol. 14, No. 4, December 2024, pp. 16-36

P- ISSN: 2220-5381
E- ISSN: 2710-1096

References

[1] J. Whaley, "An Introduction to Geomechanics", *GEO ExPro Journal*, 2019.

[2] J. Wang, and X. Ye, "A weak Galerkin finite element method for second-order elliptic problems", *Journal of Computational and Applied Mathematics*, vol. 241, pp.103-115, 2013. https://doi.org/10.1016/j.cam.2012.10.003

[3] F. Pan, K. Sepehrnoori, and L. Chin, "November. Development of a coupled geomechanics model for a parallel compositional reservoir simulator," *In SPE Annual Technical Conference and Exhibition*, *One Petro*, 2007. https://doi.org/10.2118/109867-MS

[4] A. K. Faraj, A. K. Salih, H. A. Abdul Hussein, and A. N. Abed Al-Hasnawi, "Variation of total stresses during field operation using finite element technique, Zubair oil field," *Iraqi Journal of Oil and Gas Research (IJOGR)*, vol. 3, no. 1, pp. 25–42, 2023. https://doi.org/10.55699/ijogr.2023.0301.1036

[5] A. Vedernikova, M. Parrillo, S. Akel, and D. Mardanov, "January. Overcoming Challenges in the West Qurna-2 Drilling Campaign", *In SPE/IADC Middle East Drilling Technology Conference and Exhibition*, *One Petro*, 2016. https://doi.org/10.2118/178198-MS

[6] A. K. Faraj, H. A. Abdul Hussein, and G. H. Jani,"Estimation of Static Young Modulus for the Third section in Zubair Oil Field: A Comparison Study", *Journal of Petroleum Research and Studies*, vol. 13, no. 2, pp.16-31, 2023. https://doi.org/10.52716/jprs.v13i2.693

[7] J. S. Bell, "Practical methods for estimating in situ stresses for borehole stability applications in sedimentary basins", *Journal of Petroleum Science and Engineering*, vol.38, no. (3-4), pp. 111-119, 2003. https://doi.org/10.1016/S0920-4105(03)00025-1

[8] D. Y. Ding, "Coupled simulation of near-wellbore and reservoir models", *Journal of Petroleum Science and Engineering*, vol. 76, no. (1-2), pp. 21-36, 2011. https://doi.org/10.1016/j.petrol.2010.12.004

[9] J. Zhang, "Pore pressure prediction from well logs: Methods, modifications, and new approaches", *Earth-Science Reviews*, vol. 108, no. (1-2), pp. 50-63, 2011. https://doi.org/10.1016/j.earscirev.2011.06.001

[10] B. J. Mac Donald, "Practical stress analysis with finite elements", *Glasnevin publishing*, Ireland, 2007.

[11] W. E. Pratt, and D. W. Johnson, "Local subsidence of the Goose Creek oil field", *The Journal of Geology*, vol. 34, no. 7, part 1, pp. 577-590, 1926.

Open Access
Vol. 14, No. 4, December 2024, pp. 16-36

P- ISSN: 2220-5381
E- ISSN: 2710-1096

[12] D. Kosloff, R. F. Scott, and J. Scranton, "Finite element simulation of Wilmington oil field subsidence: I. Linear modelling", *Tectonophysics*, vol. 65, no. 3-4, pp. 339-368, 1980. https://doi.org/10.1016/0040-1951(80)90082-7

[13] D. R. Allen, "Physical changes of reservoir properties caused by subsidence and repressuring operations", *Journal of Petroleum Technology*, vol. 20, no. 01, pp. 23-29, 1968. https://doi.org/10.2118/1811-PA

[14] R. F. Yerkes, and R. O. Castle, "Surface deformation associated with oil and gas field operations in the United States", *Land subsidence: proceedings of the Tokyo Symposium*, vol. 1, pp. 55-56, 1970.

[15] H. A. Merle, C. J. Kentie, G. Van Opstal, and G. M. Schneider, "Bachaquero study: a composite analysis of the behavior of a compaction drive/solution-gas drive reservoir", *(No. CONF-750924-), Shell Internat. Petr. Mij. BV*, 1975.

[16] J. B. Schoonbeek, "April. Land subsidence as a result of natural gas extraction in the province of Groningen", *In SPE European Spring Meeting, One Petro*, 1976. https://doi.org/10.2118/5751-MS

[17] T. Okumura, "Analysis of land subsidence n Nîgata", *Proc. 1st Int. Symp. on Land Subsidence, Publication 88 and 89 of the Int. Assoc. of Hydrologic Science and UNESCO*, Vol. I, p. 130, 1969.

[18] R. W. Lewis, and Y. Sukirman, "Finite element modelling for simulating the surface subsidence above a compacting hydrocarbon reservoir", *International journal for numerical and analytical methods in geomechanics*, vol. 18, no. 9, pp. 619-639, 1994. https://doi.org/10.1002/nag.1610180904

[19] M. J. Mes, "Ekofisk Reservoir Voidage and Seabed Subsidence", *Journal of Petroleum Technology*, vol. 42, vol. 11, pp. 1434-1438, 1990. https://doi.org/10.2118/19821-PA

[20] A. K. Faraj, H. Abdul Hussein, and A. Abed Al-Hasnawi, "Estimation of internal friction angle for the third section in Zubair Oil Field: A comparison study," *Iraqi Journal of Oil and Gas Research (IJOGR)*, vol. 2, no. 2, pp. 102–111, 2022. https://doi.org/10.55699/ijogr.2022.0202.1031

[21] M. Mohajjel, and C. L. Fergusson, "Dextral transpression in Late Cretaceous continental collision, Sanandaj–Sirjan Zone, western Iran", *Journal of Structural Geology*, vol. 22, no. 8, pp. 1125-1139, 2000. https://doi.org/10.1016/S0191-8141(00)00023-7

Open Access
Vol. 14, No. 4, December 2024, pp. 16-36

P- ISSN: 2220-5381
E- ISSN: 2710-1096

[22] T. Buday, S. Z. Jassim, "The regional geology of Iraq, tectonism, magmatism, and metamorphism", GEOSURV, Baghdad, Iraq,1987.

[23] H. S. Almalikee, and S. Sen. "Present-day in situ pore pressure distribution in the tertiary and cretaceous sediments of Zubair oil field, Iraq", *Asian J. Earth Sci*., vol. 13, no. 1, pp. 1-11, 2020. https://doi.org/10.3923/ajes.2020.1.11

[24] T. K. Al-Ameri, M. S. A. Jafar, and J. Pitman, "Modeling Hydrocarbon Generations of the Basrah Oil Fields, Southern Iraq", *Based on Petromod with Palynofacies Evidence, AAPG Annual Convention and Exhibition*, Houston, Texas, pp. 10-13, 2011. https://doi.org/10.3997/2214-4609-pdb.287.1176781

[25] D. L. Logan, "A first course in the finite element method", vol. 4. Thomson, 2011.

[26] S. W. Sloan, and A. J. Abbo, "Biot consolidation analysis with automatic time stepping and error control Part 1: theory and implementation", *International Journal for Numerical and Analytical Methods in Geomechanics*, vol. 23, no. 9 pp. 467-492, 1999. https://doi.org/10.1002/(SICI)1096-9853(199905)23:6%3C467::AID-NAG949%3E3.0.CO;2-R

[27] K. Terzaghi, R. B. Peck, and G. Mesri, "Soil Mechanics in Engineering Practice (2n edn)", *John wiley & sons*, New York, 1967.

[28] P. B. Bochev, and M. D. Gunzburger, "Least-squares finite element methods", *Springer Science & Business Media*, vol. 166, 2009.

[29] J. Bramble, R. Lazarov, and J. Pasciak, "A least-squares approach based on a discrete minus one inner product for first order systems", *Mathematics of Computation*, vol. 66, no. 219, pp. 935-955, 1997.

[30] Z. Cai, X. Ye, and H. Zhang, "Least-squares finite element approximations for the Reissner-Mindlin plate", *Numerical linear algebra with applications*, vol. 6, no. 6, pp. 479-496, 1999. https://doi.org/10.1002/(SICI)1099-1506(199909)6:6<479::AID-NLA172>3.0.CO;2-K

[31] P. B. Bochev, and M. D. Gunzburger, "Accuracy of least-squares methods for the Navier-Stokes equations", *Computers & fluids*, vol. 22, no. 4-5, pp. 549-563, 1993. https://doi.org/10.1016/0045-7930(93)90025-5

[32] L. Mu, J. Wang, and X. Ye, "A least-squares-based weak Galerkin finite element method for second order elliptic equations", *SIAM Journal on Scientific Computing*, vol. 39, no. 4, pp. A1531-A1557, 2017. https://doi.org/10.1137/16M1083244

Open Access
Vol. 14, No. 4, December 2024, pp. 16-36

P- ISSN: 2220-5381
E- ISSN: 2710-1096

[33] D. J. Reddish, and B. N. Whittaker, "Subsidence: occurrence, prediction and control", *Elsevier*, 2012.

[34] G. Gambolati, G. Ricceri, W. Bertoni, G. Brighenti, and E. Vuillermin, "Mathematical simulation of the subsidence of Ravenna", *Water Resources Research*, vol. 27, no. 11, pp. 2899-2918, 1991. https://doi.org/10.1029/91WR01567

[35] R. Hillis, "Pore pressure/stress coupling and its implications for seismicity", *Exploration Geophysics*, vol. 31, no. 1-2, pp. 448-454, 2000. https://doi.org/10.1071/EG00448